Electronic Supporting Information

High-Yield Alkylation and Arylation of Graphene via Grignard Reaction with Fluorographene

Demetrios D. Chronopoulos, Aristides Bakandritsos, Petr Lazar, Martin Pykal, Klára Čépe, Radek Zbořil, and Michal Otyepka*

Regional Centre for Advanced Technologies and Materials, Department of Physical Chemistry, Faculty of Science, Palacký University in Olomouc, 17. listopadu 1192/12, 771 46 Olomouc, Czech Republic.

Materials

Graphite fluoride (GF) (C:F, 1:1.1), Grignard reagents (Pentylmagnesium bromide, Allylmagnesium chloride, 4-Methoxyphenylmagnesium bromide and Ethynylmagnesium bromide) and dry tetrahydrofuran (THF) were purchased from Sigma-Aldrich. All reagents were used as received without further purification.

Experimental methods

In a typical Grignard reaction, graphite fluoride (GF, 30 mg) was suspended in 10 mL of dry THF with the aid of sonication for 4 h and the mixture was vacuum-degassed and back-filled with nitrogen three times. Subsequently, the Grignard reagent (5 mmol) was added dropwise through a septum to the above suspension and the reaction mixture was stirred under nitrogen for 5 h. Then, the unreacted Grignard reagent was quenched with saturated aqueous solution of ammonium chloride (NH_4Cl), the organic «black» layer was collected and the solution was centrifuged for 10 min at 15000 rounds per min. The black precipitate was repeatedly suspended in water and separated by centrifugations. In order to remove any magnesium salt residues, the material was re-suspended in a solution of 5% HCl and the solution was centrifuged as previously. Finally, the precipitate was washed consecutively with water, ethanol and dichloromethane several times and the desired material was collected after centrifugation.

To ensure adequate purification of the washed conjugated products, their FT-IR spectra were recorded, and they were then subjected to the washing procedures described above once again. After this second washing, their FT-IR spectra were recorded and compared to those obtained after the first wash. This procedure was repeated until the spectra from the products after two successive washes exhibited no detectable differences in the relative intensities of their various bands. At this point the products were considered to be pure, with no residual non-covalently bound reagents.

The optical band gap values were assessed using the Tauc plot approach [1] based on the equation:

$$ahv = b(hv - E_g)^n,$$

where a is the absorption coefficient, hv is the photon energy, E_g is the optical band gap (OBG), n=0.5 for direct transitions, and b is a constant. We have selected n=0.5 because our DFT calculation revealed that the band gap is direct for all functionalized graphenes. The linear part of the plot of

$(ahv)^2$ versus hv and extrapolation to zero (ahv) may provide the OBGs. Tauc plots have been extensively used for the estimation of the OBG of 2D materials such as graphene derivatives,[2] GO and reduced GO,[3] phosphorene,[4] and boron nitride.[5] Linear parts can be found in more than one energy region, therefore some rational for selecting the energy region is necessary. The low energy regions have been used when low energy OBG are expected, such as in the case of reduced GO[3] or phosphorene.[4] In the present case, given the suggestion from the theoretical calculations and the black color of the graphene derivatives, we selected the lower experimentally available energies to extract the optical band gaps.

Theoretical calculations

The partial atomic charges of individual atoms of alkyl- and aryl- anions were obtained from a restrained electrostatic potential (RESP) fit procedure[6] on the level B3LYP/aug-cc-pVTZ using the Gaussian 03 (rev. E.01) software.[7] The geometries were optimized at the same level of theory.

The Density Functional Theory (DFT) calculations on graphene were performed using the projector-augmented wave (PAW) method in the Vienna Ab initio Simulation Package (VASP) suite.[8,9] The PBE functional was employed to account for exchange-correlation effects.[10] In order to mimic the high density of functional groups on graphene as experimentally observed, the graphene sheet was modeled using a 2×3 supercell (12 carbon atoms) with a calculated C-C bond length of 1.44 Å. The allyl-, pentyl-, and methoxyphenyl groups were placed on both sides of graphene sheet, which resulted in the 1:6 coverage of graphene (one molecular group per six carbon atoms of graphene). The groups were attached to neighboring carbon atoms, as this adsorption geometry minimizes the strain of the graphene lattice due to the sp^3 coordination change of carbon atoms bonded to the groups. The periodically repeated functionalized layers were separated by 20 Å of vacuum. The energy cutoff for the plane-wave expansion was set to 400 eV and 8×6×1 *k*-point grid was used. The density of states was calculated with dense *k*-point grid of 24×18×1 *k*-points. The binding energy was calculated as the difference between the energy of the most favorable configuration of the complex (allyl-, pentyl-, and methoxyphenyl groups bonded to graphene) and the sum of the energies of the respective isolated species.

Calculation of the degree of functionalization

In order to calculate the functionalization degrees, we combined the information provided both from TGA and XPS techniques. According to this rational, the mass % of the functional groups [m_{fn}] was considered equal to the mass % loss from TGA [m_{loss}] after subtracting the mass % of the impurities (N,O and F), as estimated from XPS analysis. The mass % of the rest of the graphene material (lattice carbons and impurities) was considered equal to: m_{graph}= 100 - m_{fn}. Then, the molar percentages were calculated for m_{fn} and m_{graph}. In the latter case, calculation of the molar % for m_{graph} was possible because the mass % of the lattice carbons [$m_{C\text{-}lat}$] and of the N, O and F impurities could be separately calculated from XPS analysis. The molar % of the lattice carbons [$m_{C\text{-}lat}/12$] was considered equal to the total at. % in carbon (from XPS) minus the mole % of the carbon atoms of the functional groups (estimated from m_{fn}). Therefore, the functionalization degree was calculated based on the formula:

$$\text{F.D} = \frac{mol_{fn}}{mol_{graph}} = \frac{m_{fn}/M_{w,f}}{m_{C-lat}/12 + m_N/14 + m_O/16 + m_F/19},$$

where moles and masses are percentages and $M_{w,f}$ is the molecular weight of the functional group. For the case of the anisol derivative, the oxygen content was ascribed to 5% O impurities (since the other two derivatives also contained 5% O impurities) and the rest 3.3 % ascribed to the oxygen atoms from anisol. It is interesting to note that based only on the 3.3 at. % of O as obtained from XPS, the calculated degree of functionalization is:

$$\frac{mol_{anisol}}{mol_{graph}} = \frac{3.3}{100 - 3.3\times 8}\times 100 = 4.5,$$

where mol_{anisol} is the mol % of anisol groups and which equals the at % of anisol oxygen (3.3 at.%) and mol_{graph} is the mol % of the rest of the atoms of the material, which do not belong to anisol (lattice C atoms, O, N, and F impurities). 3.3×8 is the total number of detected atoms by XPS in the anisol groups. This DF is very close to the one calculated from the combined TGA and XPS analysis and reported in the main manuscript, according to the rational explained previously.

The mass losses of the functional groups were determined from the weight losses recorded on TGA up to 580 °C (45% for PeG, 42.5% for AlG, and 44% for AnG). Taking into account that XPS analysis showed the presence of fluoro and oxygen atoms in all materials, their masses were subtracted from the mass loss during TGA, according to the rational explained in the previous paragraph.

Instrumentation

Raman spectra and AFM images were recorded on NTEGRA Spectra S (NT-MDT) microscope using the 532 nm excitation line of a diode laser. The spectra were accumulated for 600 s (with 1s exposition time) employing 50 μm slit, grating of 600 lines/mm, and thermoelectrically cooled detector.

X-ray photoelectron spectroscopy (XPS) was performed with Phoibos 100 spectrometer.

FT-IR spectra were recorded on an iS5 FTIR spectrometer (Thermo Nicolet) with the Smart Orbit ZnSe ATR technique. ATR and baseline corrections were applied to the collected spectra.

Thermogravimetric analysis (TGA) with evolved gas analysis (EGA) was performed using a Netzsch STA 449C Jupiter, coupled with a quadrupole mass spectrometer QMS 403C Aëolos. The measurements were carried out in an open crucible from α-Al_2O_3 in N_2 flow. A temperature program from 40 to 1000 °C with heating rate 10 °C min^{-1} was used. Before each experiment, the crucibles were heated to 1340 °C and then cooled to room temperature. The masses in the range of 12-100 *m/z* of the released gases for the PeG graphene derivative were determined with the mass spectrometer of the TGA instrument, starting at 100 °C to avoid overloading the spectrometer with adsorbed water.

Microscopic images were obtained by TEM JEOL 2010 with LaB6 type emission gun, operating at 160 kV. STEM-HAADF (high-angle annular dark-field imaging) analyses for EDS (energy-dispersive X-ray spectroscopy) mapping of elemental distributions on the products were performed with a FEI Titan HRTEM microscope operating at 80 kV.

Supplementary Figures

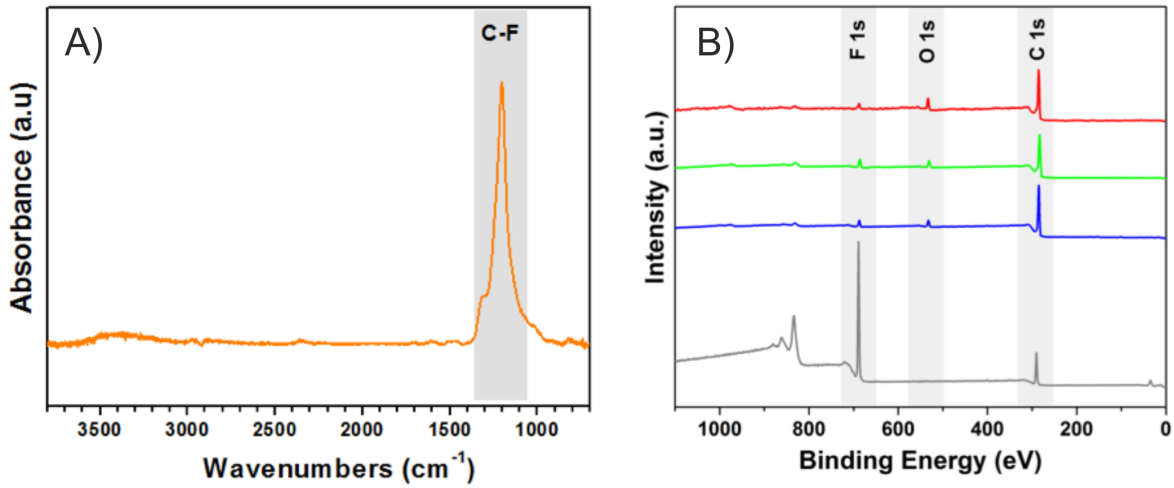

Figure S1. FT-IR spectrum of pristine GF (A). XPS survey spectra of pristine GF (grey) and pentyl- (blue), allyl- (green) and anisolyl-functionalized (red) graphenes (B).

Table S1. Elemental composition of chemically modified graphenes and pristine graphite fluoride (GF) as obtained from the XPS analyses (wide scan XPS spectra).

	Atomic percentage [%]			
	C 1s (283 eV)	**O 1s** (531 eV)	**N1s** (686 eV)	**F 1s** (686 eV)
PeG	90.6	5.2	<1	3.7
AlG	88.8	5.2	<1	5.4
AnG	88.1	8.3	<1	3.1
GF	43.5	<1	-	55.7

Table S2. Determination of the different carbon components obtained from the deconvolution of the high resolution C1s XPS spectra of the chemically modified graphenes and of the pristine GF.

	Carbon components [%]					
	C=C (284.8-284.7 eV)	**C-C** (285.8-285.2 eV)	**C-O** (286.6-286.5 eV)	**C*-CF** (287.72-287.3 eV)	**CF** (290.3-289.6 eV)	**CF_2/ C^*F_2-CF_X/ CF_3** (294.0-289.6 eV)
PeG	48.2	38.4[a]	6.8	3.6	3.0	-
AlG	62.9	17.9[a]	5.2	9.4	4.6	-
AnG	68.1	6.5[a]	15.8	5.3	4.2	-
GF	<1	<1	-	2.3	78[b]	18.0

[a]The % of the C-C (sp^3) components nicely corroborate the structure of the covalently attached groups. Accordingly, for the pentyl-graphene the highest C-C content is observed, while for the anisolyl- the lowest. [b]In the case of GF, this component corresponds mainly to CF-CF bonds.

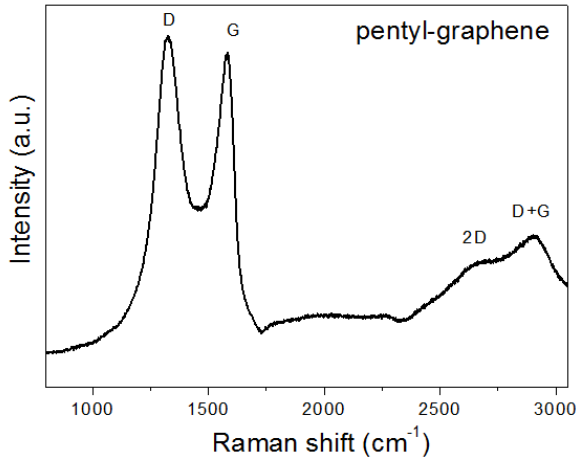

Figure S2. Raman spectrum showing the 2D band of the pentyl graphene derivative. The FWHM, the symmetry and deconvolution of the 2D Raman band can provide information on the number of graphene layers.[11,12] For the case of highly functionalized graphene derivatives the situation changes since there is very high broadening of the Raman bands (including the 2D), which does not allow extraction of the information from the 2D band.[11, 32 (in the main text)]

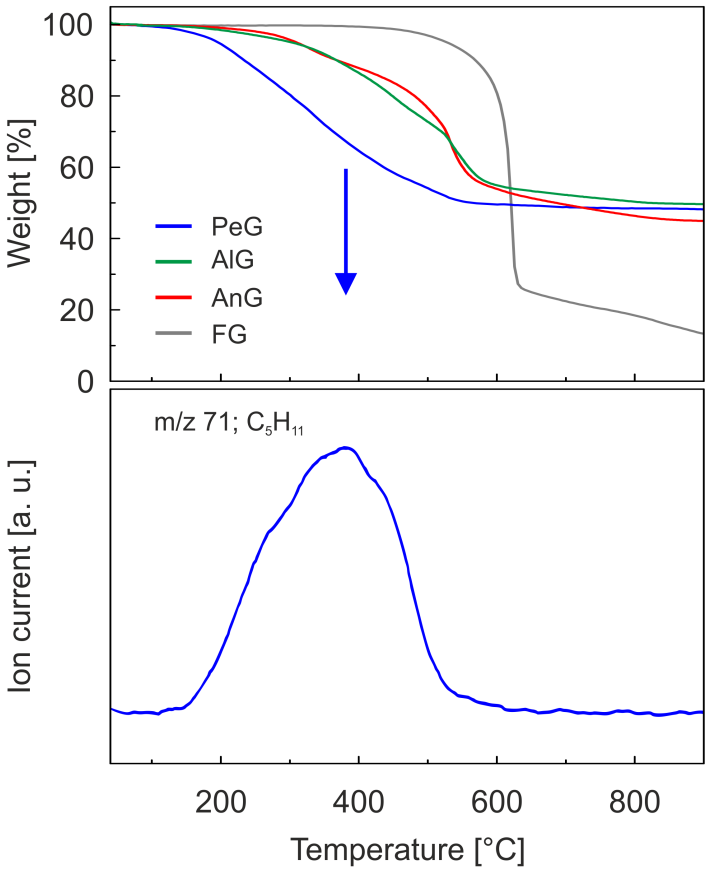

Figure S3. TGA graphs of graphite fluoride (grey) and pentyl (blue), allyl (green) and anisol graphene (red), obtained under inert N_2 atmosphere. Ion current vs. temperature curve obtained with a mass spectrometer during the thermal degradation study (TGA-MS) of the pentyl-graphene derivative.

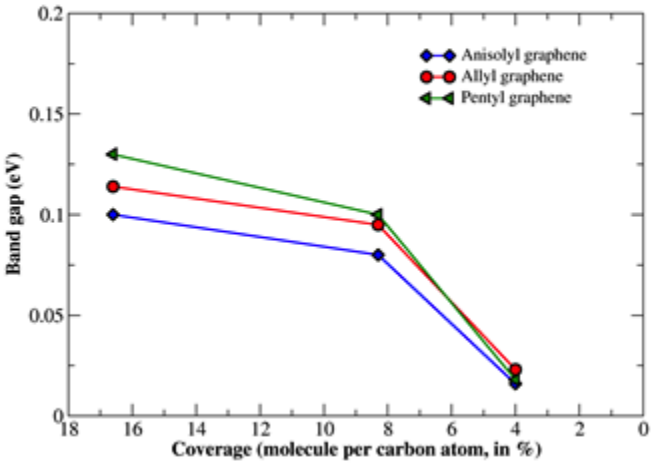

Figure S4. The electronic band gap of functionalized graphenes as a function of coverage. Coverage "0" represents pristine graphene.

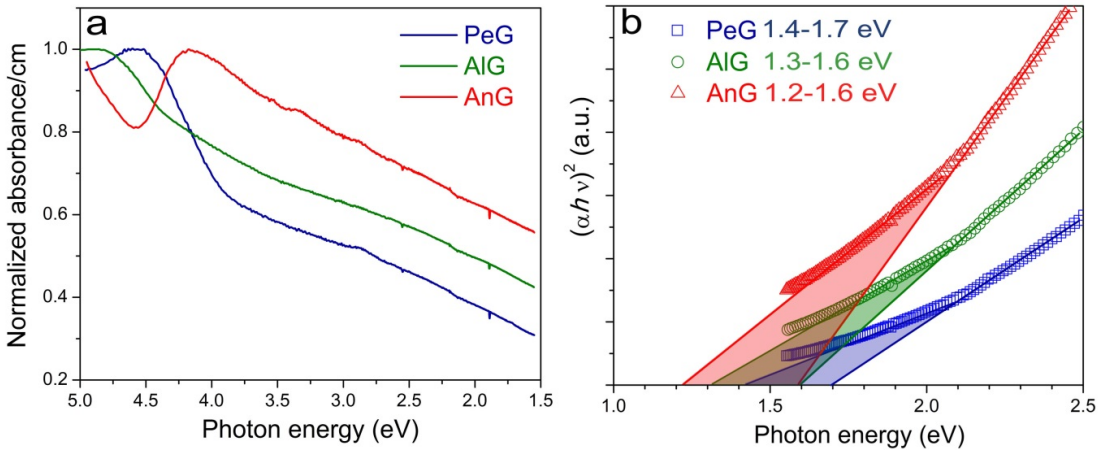

Figure S5. (a) Absorbance spectra of the graphene derivatives in the energy window of 5-1.5 eV (250-800 nm) and (b) Tauc plots thereof in the low energy region. At these energies, two linear parts in the graphs were identified, which have been both used. Extrapolation to the x-axis suggests a window for the possible OBG values of the three products, as shown in the graph.

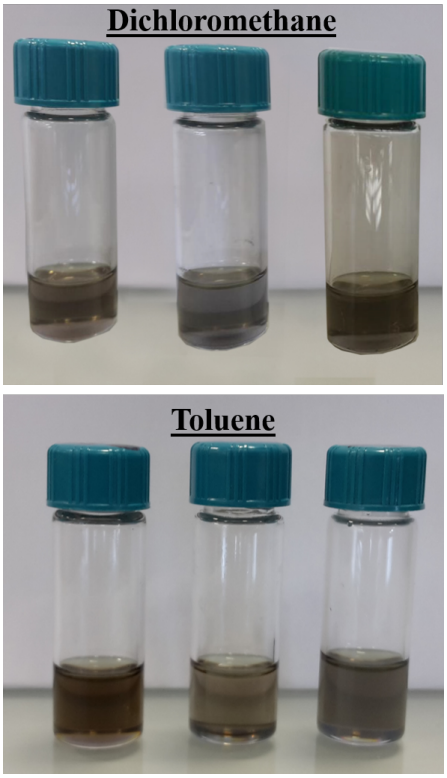

Figure S6. Digital images of alkyl-, alkenyl-, and aryl-functionalized graphenes dispersed in dichloromethane and in toluene (the vials in the photographs appear with the same order as the derivatives referred in the text). The materials were sonicated in the solvent for 1 h and rested for 18 h before capturing the images.

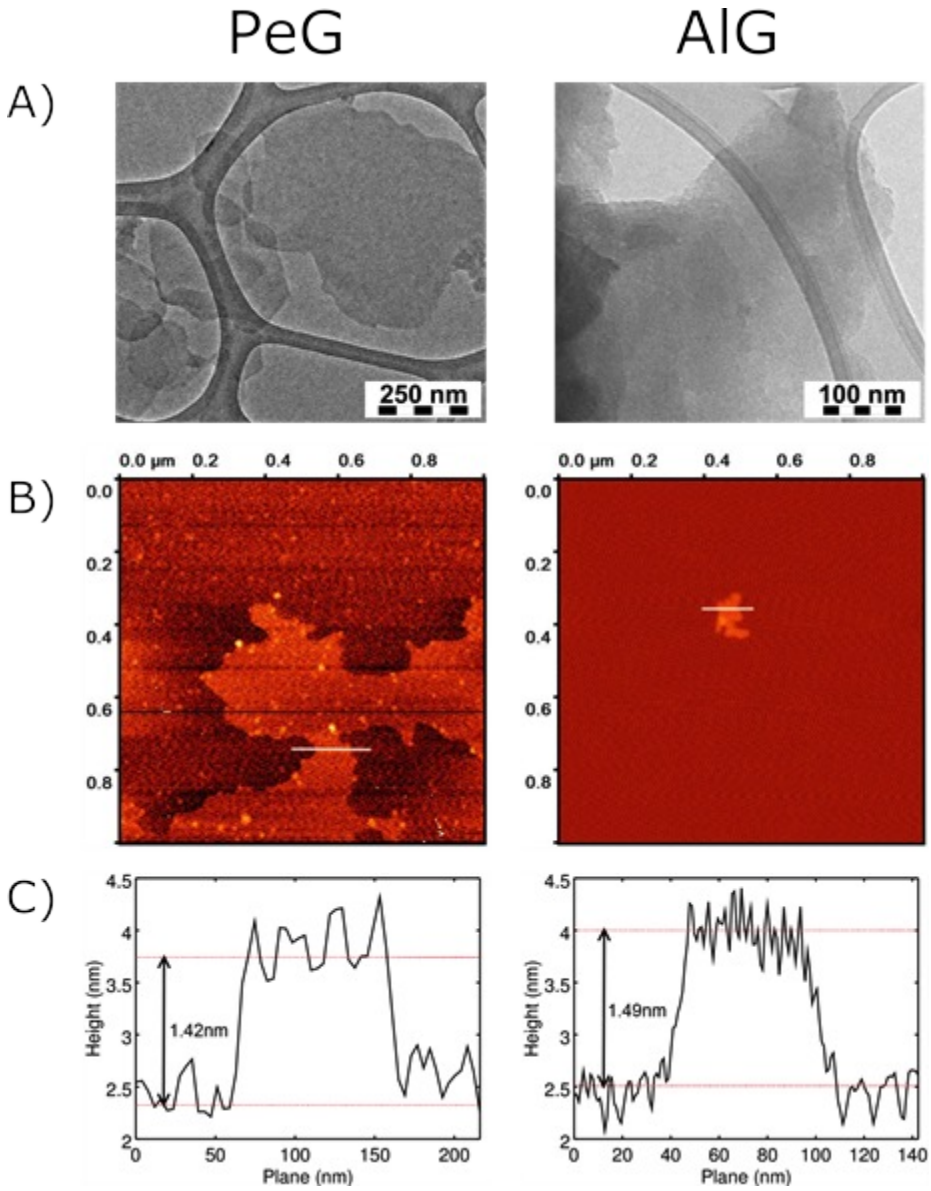

Figure S7. TEM (A) and AFM images (B) of PeG and AlG on freshly prepared mica substrates and their height profiles (C).

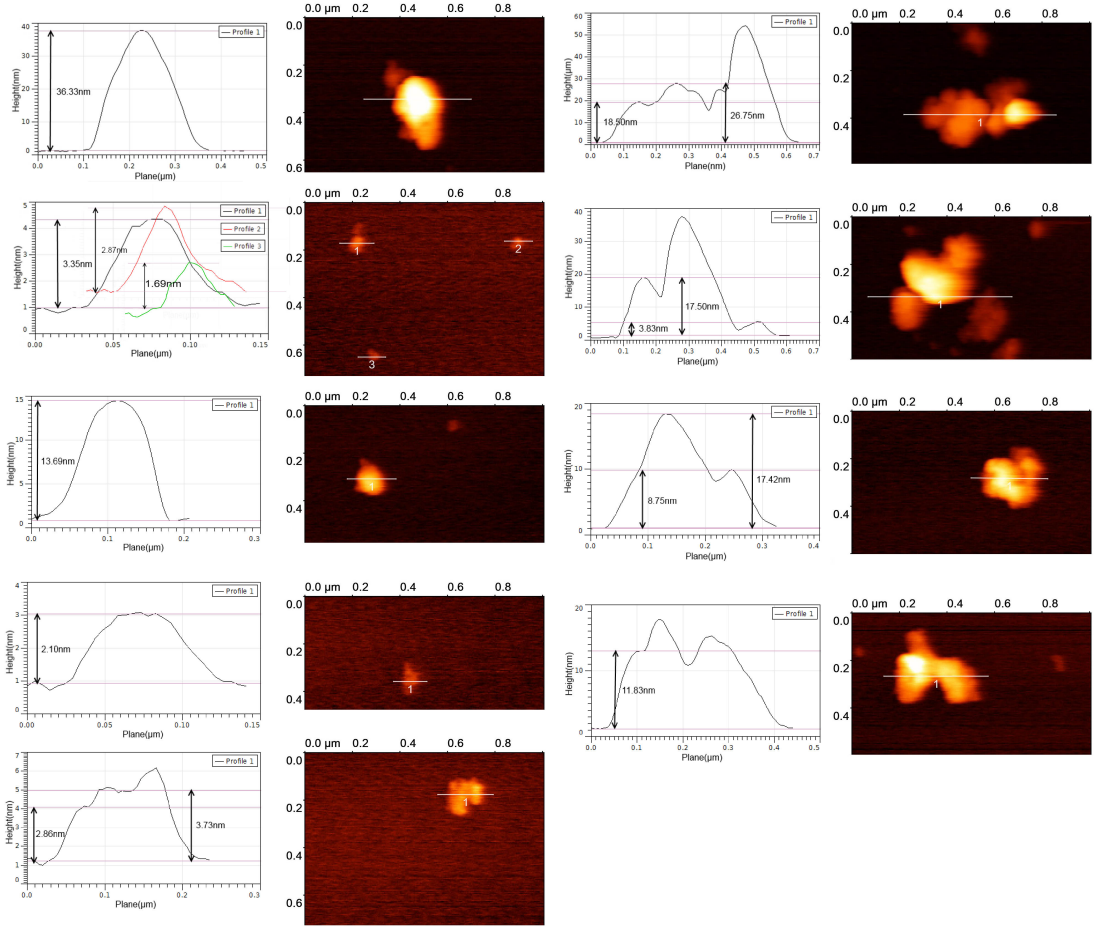

Figure S8. Several AFM images and height profiles of flakes from the AlG product, verifying the few layer nature of the derivative.

(1) Tauc, J. Optical Properties and Electronic Structure of Amorphous Ge and Si. *Mater. Res. Bull.* **1968**, *3* (1), 37–46.

(2) Capasso, A.; Salamandra, L.; Faggio, G.; Dikonimos, T.; Buonocore, F.; Morandi, V.; Ortolani, L.; Lisi, N. Chemical Vapor Deposited Graphene-Based Derivative As High-Performance Hole Transport Material for Organic Photovoltaics. *ACS Appl. Mater. Interfaces* **2016**, *8*, 23844–23853.

(3) Mathkar, A.; Tozier, D.; Cox, P.; Ong, P.; Galande, C.; Balakrishnan, K.; Leela Mohana Reddy, A.; Ajayan, P. M. Controlled, Stepwise Reduction and Band Gap Manipulation of Graphene Oxide. *J. Phys. Chem. Lett.* **2012**, 3, 986–991.

(4) Woomer, A. H.; Farnsworth, T. W.; Hu, J.; Wells, R. A.; Donley, C. L.; Warren, S. C. Phosphorene: Synthesis, Scale-Up, and Quantitative Optical Spectroscopy. *ACS Nano* **2015**, *9*, 8869–8884.

(5) Song, L.; Ci, L.; Lu, H.; Sorokin, P. B.; Jin, C.; Ni, J.; Kvashnin, A. G.; Kvashnin, D. G.; Lou, J.; Yakobson, B. I.; Ajayan, P. M. Large Scale Growth and Characterization of Atomic Hexagonal Boron Nitride Layers. *Nano Lett.* **2010**, *10* (8), 3209–3215.

(6) Bayly, C. I.; Cieplak, P.; Cornell, W. D.; Kollman, P. A. A Well-Behaved Electrostatic Potential Based Method Using Charge Restraints for Deriving Atomic Charges: The RESP Model. *J. Phys. Chem.* **1993**, *97*, 10269–10280.

(7) Frisch, M. J.; Trucks, G. W.; Schlegel, H. B.; Scuseria, G. E.; Robb, M. A.; Cheeseman, J. R.; Montgomery, Jr., J. A.; Vreven, T.; Kudin, K. N.; Burant, J. C.; Millam, J. M.; Iyengar, S. S.; Tomasi, J.; Barone, V.; Mennucci, B.; Cossi, M.; Scalmani, G.; Rega, N.; Petersson, G. A.; Nakatsuji, H.; Hada, M.; Ehara, M.; Toyota, K.; Fukuda, R.; Hasegawa, J.; Ishida, M.; Nakajima, T.; Honda, Y.; Kitao, O.; Nakai, H.; Klene, M.; Li, X.; Knox, J. E.; Hratchian, H. P.; Cross, J. B.; Bakken, V.; Adamo, C.; Jaramillo, J.; Gomperts, R.; Stratmann, R. E.; Yazyev, O.; Austin, A. J.; Cammi, R.; Pomelli, C.; Ochterski, J. W.; Ayala, P. Y.; Morokuma, K.; Voth, G. A.; Salvador, P.; Dannenberg, J. J.; Zakrzewski, V. G.; Dapprich, S.; Daniels, A. D.; Strain, M. C.; Farkas, O.; Malick, D. K.; Rabuck, A. D.; Raghavachari, K.; Foresman, J. B.; Ortiz, J. V.; Cui, Q.; Baboul, A. G.; Clifford, S.; Cioslowski, J.; Stefanov, B. B.; Liu, G.; Liashenko, A.; Piskorz, P.; Komaromi, I.; Martin, R. L.; Fox, D. J.; Keith, T.; Al-Laham, M. A.; Peng, C. Y.; Nanayakkara, A.; Challacombe, M.; Gill, P. M. W.; Johnson, B.; Chen, W.; Wong, M. W.; Gonzalez, C.; Pople, J. A. Gaussian 03, Revision E.01; Gaussian, Inc.: Wallingford, CT, **2004**

(8) Blochl, P. E., Projector Augmented-wave Method. *Physical Review B* **1994,** *50* (24), 17953-17979.

(9) Kresse, G.; Joubert, D., From ultrasoft pseudopotentials to the projector augmented-wave method. *Physi. Review B* **1999,** *59*, 1758-1775.

(10) Perdew, J. P.; Burke, K.; Ernzerhof, M., Generalized gradient approximation made simple (vol 77, pg 3865, 1996). *Phys.Rev.Lett.* **1997,** *78*, 1396-1396.

(11) Englert, J. M.; Dotzer, C.; Yang, G.; Schmid, M.; Papp, C.; Gottfried, J. M.; Steinrück, H.-P.; Spiecker, E.; Hauke, F.; Hirsch, A. Covalent Bulk Functionalization of Graphene. *Nat. Chem.* **2011**, *3*, 279–286.

(12) Hao, Y.; Wang, Y.; Wang, L.; Ni, Z.; Wang, Z.; Wang, R.; Koo, C. K.; Shen, Z.; Thong, J. T. L. Probing Layer Number and Stacking Order of Few-Layer Graphene by Raman Spectroscopy. *Small* **2010**, *6* (2), 195–200.